

# Hierarchical Conformal Classification

Floris den Hengst<sup>1</sup>, Inès Blin<sup>1,2</sup>, Majid Mohammadi<sup>1</sup>, Syed Ihtesham Hussain Shah<sup>1</sup>, Taraneh Younesian<sup>1</sup>

<sup>1</sup>Vrije Universiteit Amsterdam, Amsterdam, The Netherlands

<sup>2</sup>Sony Computer Science Laboratories - Paris, Paris, France

{f.den.hengst, i.blin, s.i.h.shah, t.younesian}@vu.nl, majid.mohammadi690@gmail.com

## Abstract

Conformal prediction (CP) is a powerful framework for quantifying uncertainty in machine learning models, offering reliable predictions with finite-sample coverage guarantees. When applied to classification, CP produces a prediction set of possible labels that is guaranteed to contain the true label with high probability, regardless of the underlying classifier. However, standard CP treats classes as flat and unstructured, ignoring domain knowledge such as semantic relationships or hierarchical structure among class labels. This paper presents *hierarchical conformal classification (HCC)*, an extension of CP that incorporates class hierarchies into both the structure and semantics of prediction sets. We formulate HCC as a constrained optimization problem whose solutions yield prediction sets composed of nodes at different levels of the hierarchy, while maintaining coverage guarantees. To address the combinatorial nature of the problem, we formally show that a much smaller, well-structured subset of candidate solutions suffices to ensure coverage while upholding optimality. An empirical evaluation on three new benchmarks consisting of audio, image, and text data highlights the advantages of our approach, and a user study shows that annotators significantly prefer hierarchical over flat prediction sets.

## Introduction

Conformal prediction (CP) is a powerful tool for estimating and representing the uncertainty of predictive models, which is crucial in high-stakes application domains (Vovk, Gammerman, and Shafer 2005; Angelopoulos, Bates et al. 2023). CP provides statistical guarantees for any model that outputs prediction scores in a finite-sample regime. For a given input, it produces a set of predictions that contain the ground truth at a user-specified confidence level. This property of CP is known as its *coverage* guarantee.

Motivated by the adoption and success of CP, approaches have been proposed that display additional desiderata on top of its key *coverage* property. Examples include approaches that provide a coverage guarantee conditional to the input (Angelopoulos et al. 2021), those that incorporate different misclassification costs for different classes using a risk control framework (Angelopoulos et al. 2024), and methods that produce structured prediction sets (Wieslander et al. 2020; Zhang, Li, and Bastani 2025).

However, relatively little attention has been paid to incorporating prior domain knowledge into the process of gen-

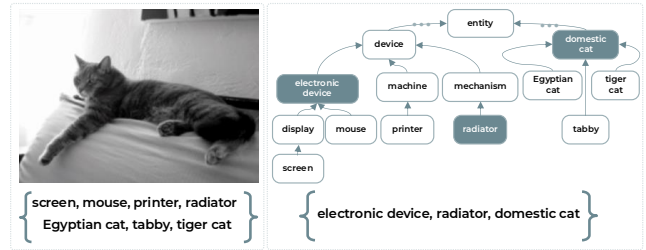


Figure 1: Input with standard CP output (left), hierarchy subset with compact hierarchy-informed output (right).

erating prediction sets with coverage guarantees. For classification, the semantics of a particular domain are often captured in a taxonomy or hierarchical organization among class labels. The directed acyclic graph (DAG) is the dominant modeling paradigm for doing so. Examples include the organization of diseases in diagnosis (Zesch and Gurevych 2007), fraud types in fraud detection (Bennett 2013), and article types in text classification (Zesch and Gurevych 2007). Another well-known example is ImageNet (Russakovsky et al. 2015), where class labels are derived from the WordNet lexical database (Miller 1995). Figure 1 exemplifies how class hierarchies are crucial to creating prediction sets that are more compact, better aligned with how end users understand the domain, and thereby more useful.

While recent studies have incorporated hierarchies in labels into the prediction sets (Angelopoulos et al. 2024; Zhang, Li, and Bastani 2025), they fail to balance between the compactness of the prediction sets and their specificity. We propose *Hierarchical Conformal Classification (HCC)*, an extension of conformal prediction that incorporates class hierarchies into the structure of prediction sets. Rather than treating labels as flat and unstructured, HCC leverages a given class taxonomy modeled as a DAG to construct sets containing nodes from different levels of the taxonomy—including both fine-grained leaf classes and more general ancestor nodes. HCC formulates the construction of such sets as a constrained optimization problem: among all subsets of the hierarchy that guarantee the required coverage, it selects one that minimizes the size of the prediction set while maximizing its specificity.

Our solution is inspired by the learn-then-test approach by Angelopoulos et al. (2025), and combines learning with search. Our search step is efficient and scalable because it is conducted over a carefully constructed subspace of candidate solutions. We show that, despite the combinatorial nature of search over the whole hierarchy, it suffices to search within this much smaller, well-structured subset of candidates. Crucially, HCC preserves the finite-sample coverage guarantees of standard CP by ensuring that the true label is always included in the leaf-level coverage of the returned set. By allowing for the replacement of many similar leaf classes with a single general parent, HCC provides more compact and usable predictions that are better aligned with how users understand the label space.

The contributions of this paper can be summarized as:

- We formalize *Hierarchical Conformal Classification (HCC)* as an extension of conformal prediction that accounts for the hierarchy among class labels, formalizing the prediction set construction as a constrained optimization problem with labels in a DAG.
- We design efficient calibration and inference algorithms for HCC, including a search-based procedure that exploits the structure of the hierarchy to solve the optimization problem with guaranteed coverage.
- We present and release<sup>1</sup> three use cases and benchmarks that span multiple data modalities - audio, image, and text - where class hierarchies are available, and we demonstrate the effectiveness of HCC through both quantitative evaluation and a user study.

HCC thereby bridges structured prediction and uncertainty quantification, with broad applicability across domains, offering a foundation for more reliable and user-aligned classification systems.

## Related Work

A handful of works have recently explored prediction sets in hierarchical label spaces, but HCC differs fundamentally in both goal and methodology. Prior methods, such as Mortier et al. (2022, 2025), aim to capture regions of high probability mass and are limited to trees, rather than our more general focus on coverage guarantees for DAGs. Angelopoulos et al. (2024) focuses on bounding the hierarchical distance rather than achieving leaf coverage, and their approach restricts the inference strictly to ancestor nodes of the most likely label. In contrast, our approach can flexibly include both internal and leaf nodes based on a user-specified trade-off between prediction set size and specificity. Zhang, Li, and Bastani (2025) adopt a learn-then-test framework to achieve a similar goal to ours, and provides coverage guarantees, but their method requires a user-specified limit on the nominal prediction set size and relies on an integer programming formulation that may not scale well with the taxonomy size. In contrast, our approach allows for explicit balancing of compactness with specificity and introduces a structured and

<sup>1</sup><https://github.com/florisdhengst/hierarchical-conformal-classification>

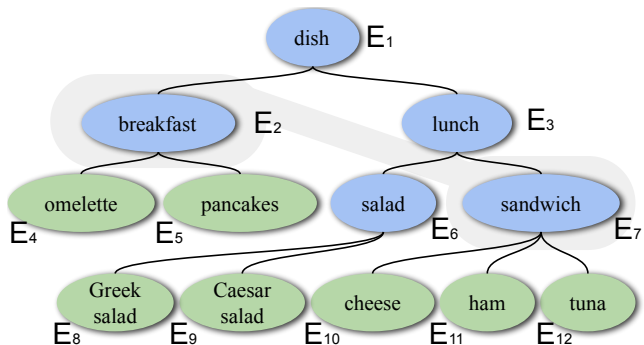


Figure 2: Taxonomy for the running example.

substantially reduced search during calibration, which is further pruned of spurious solutions during inference in a scalable way. Wieslander et al. (2020) combine deep learning with conformal prediction for the classification of subregions of tissues. They assess region-specific drug response by employing hierarchical identification of tissue regions and measuring confidence in subregion detection. However, this approach is specific to this problem domain and does not use an existing class hierarchy.

## Background

**Notation.** We use calligraphic letters (e.g.  $\mathcal{X}, \mathcal{F}$ ) to denote sets, capital letters (e.g.,  $X, Y$ ) for random variables, and bold lowercase letters (e.g.,  $\mathbf{x}$ ) for deterministic vectors. Bold uppercase letters (e.g.,  $\mathbf{X}$ ) denote matrices. We focus on multi-class classification problems, where the input space is  $\mathcal{X} \subset \mathbb{R}^d$ , and the label space is  $\mathcal{Y} = \{1, \dots, k\}$ . A trained predictive model is denoted by  $\hat{f} \in \mathcal{F}$ , where  $\hat{f} : \mathcal{X} \rightarrow [0, 1]^k$  and  $\sum_{i=1}^k \hat{f}(\mathbf{x})_i = 1$ . That is, given an input  $\mathbf{x} \in \mathcal{X}$ , the model outputs a prediction score, which can be a probability distribution, over the  $k$  classes. We denote the calibration and test data sets as  $\mathcal{D}_c$  and  $\mathcal{D}_t$ , respectively. Each set contains  $n_c$ , respectively  $n_t$ , data pairs  $(\mathbf{x}_i, y_i)$ , where  $y_i \in \mathcal{Y}$ .

## Conformal prediction

CP equips any probabilistic classifier with a finite-sample *coverage guarantee* that a prediction will contain the correct label with probability at least  $1 - \alpha$ . Given a test input  $\mathbf{x}_t \in \mathcal{D}_t$  and a desired maximum error rate  $\alpha \in [0, 1)$ , CP returns a prediction set  $\mathcal{Y}' \subseteq \mathcal{Y}$  such that:

$$\mathbb{P}(y_t \in \mathcal{Y}') \geq 1 - \alpha, \quad (1)$$

where  $y_t \in \mathcal{Y}$  is the true label of  $\mathbf{x}_t$ .

We adopt the standard *split conformal prediction* approach in which the goal is to find some conformal predictor  $h_{\mathcal{Y}} \in \mathcal{X} \times [0, 1) \rightarrow 2^{\mathcal{Y}}$ . A fixed model  $\hat{f}$  is calibrated using a separate calibration set  $\mathcal{D}_c = \{(\mathbf{x}_i, y_i)\}_{i=1}^{n_c}$ , and a *conformity score*  $s \in \mathcal{X} \times \mathcal{Y} \rightarrow \mathbb{R}$ . An example of this score is the predicted value of class  $y$  for input  $\mathbf{x}$ , i.e.,  $s(\mathbf{x}, y) := \hat{f}(\mathbf{x})_y$ . For each instance in the calibration set, CP computes the conformity score  $s(\mathbf{x}_i, y_i)$ , resulting in the

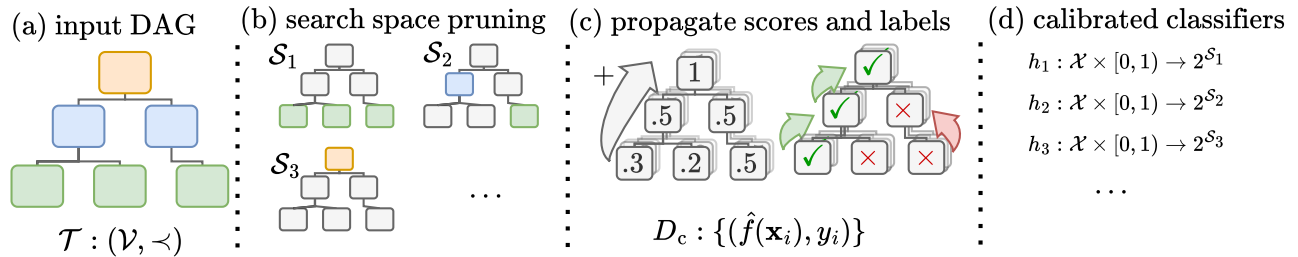


Figure 3: Visualization of HCC training: (a) for an input DAG with nodes  $\mathcal{V}$ , (b) a set of subsets that each cover all leaf nodes is derived. These are referred to as the *leaf covers*. (c) Prediction scores  $\hat{f}(X)$  and ground truth labels  $Y$  in a calibration set  $D_c$  are propagated up the taxonomy, and (d) used to calibrate a set of conformal classifiers, one for each leaf cover. Each of these conformal classifiers takes as input a desired error level  $\alpha \in [0, 1)$  and the propagated prediction scores for its leaf cover, and outputs a subset of this leaf cover as its prediction.

set  $\mathcal{S} = \{s(\mathbf{x}_i, y_i)\}_{i=1}^{n_c}$ . Next, the quantile  $\hat{q}$  of the empirical distribution of  $\mathcal{S}$  is determined so that the desired coverage ratio  $1 - \alpha$  is achieved by choosing  $\hat{q} = \lceil (n+1)(1-\alpha) \rceil / n$  where  $\lceil \cdot \rceil$  denotes the ceiling function<sup>2</sup>. At inference time, the prediction set is constructed as

$$C(\mathbf{x}_t) := \{y \in \mathcal{Y} : s(\mathbf{x}_t, y) \geq \hat{q}\}. \quad (2)$$

## Hierarchies

We assume that the classes are organized in a hierarchy, modeled as a DAG  $\mathcal{T} := (\mathcal{V}, \prec)$  of depth  $\delta$ . The node set  $\mathcal{V}$  contains all hierarchical class labels, and the base classifier classes correspond to the set of leaves  $\mathcal{Y} \subseteq \mathcal{V}$ . The edge relation  $\prec$  denotes the strict “parent-of” relationship, satisfying asymmetry, anti-reflexivity, and transitivity.

**Definition 1** (Hierarchy). *Let  $\mathcal{T} = (\mathcal{V}, \prec)$  be a DAG where  $\prec$  is a strict partial order. We refer to  $\mathcal{T}$  as a class hierarchy over nodes  $\mathcal{V}$ .*

We denote the transitive closure of  $\prec$  by  $\ll$ . The hierarchy has a unique root node  $\text{root} \in \mathcal{V}$  such that  $\nexists v \in \mathcal{V}$  with  $\text{root} \prec v$ .

**Definition 2** (Leaves). *Let  $\mathcal{T} = (\mathcal{V}, \prec)$  be a hierarchy. The set of leaves—i.e., the classification labels—is defined as:*

$$\text{leaves}(\mathcal{T}) := \{v \in \mathcal{V} \mid \nexists w \in \mathcal{V} \text{ such that } w \prec v\}.$$

We assume  $\mathcal{Y} = \text{leaves}(\mathcal{T})$ .

**Definition 3** (Lowest Common Ancestor, LCA). *Let  $\mathcal{T}$  be as in Definition 1, and let  $\ll$  denote the transitive closure of  $\prec$ . For a non-empty set of nodes  $\mathcal{S} \subseteq \mathcal{V}$ , define the set of common ancestors as:*

$$\text{Anc}_{\mathcal{T}}(\mathcal{S}) := \{a \in \mathcal{V} \mid \forall v \in \mathcal{S}, a \ll v\}.$$

The lowest common ancestor(s) of  $\mathcal{S}$ , denoted  $\text{LCA}_{\mathcal{T}}(\mathcal{S})$ , is the set of minimal elements in  $\text{Anc}_{\mathcal{T}}(\mathcal{S})$  with respect to  $\ll$ :

$$\text{LCA}_{\mathcal{T}}(\mathcal{S}) := \{a^* \in \text{Anc}_{\mathcal{T}}(\mathcal{S}) \mid \nexists a' \in \text{Anc}_{\mathcal{T}}(\mathcal{S}) : a^* \ll a'\}.$$

As a running example, we consider a classification problem over 7 dish types in Figure 2. It consists of twelve nodes in a DAG of depth four, with seven leaves highlighted in green. These leaves correspond to the classification labels. lunch is the lowest common ancestor of {Caesar salad, cheese sandwich}.

<sup>2</sup>this is essentially the  $\hat{q}$  quantile with a minor adjustment

## Hierarchical Conformal Classification

### Formulation

We consider the problem of producing compact and informative prediction sets with coverage guarantees, under the assumption that class labels are structured according to a known DAG. Each prediction set should ideally contain a small number of nodes to promote usability and avoid redundancy. Moreover, each leaf represents a concrete class label, and the prediction of an internal node with many leaves as its descendants implies greater uncertainty of the base classifier. Therefore, the nodes in the prediction set should have a small number of leaves as descendants. Thus, compact prediction sets that have a small number of leaves as descendants provide more specific and actionable predictions. These objectives must be achieved while still satisfying the standard conformal prediction coverage guarantee to ensure the reliability of the prediction.

To formalize these desiderata, we introduce the notion of a leaf cover, which quantifies the implied coverage of class nodes for a set of arbitrary nodes  $\mathcal{N}$ . Returning to our running example in Figure 2, the set {breakfast, sandwich} has leaf cover {omelette, pancakes, cheese sandwich, ham sandwich, tuna sandwich}.

**Definition 4** (Leaf Cover). *For any subset  $\mathcal{N} \subseteq \mathcal{V}$  of a DAG  $\mathcal{T} = (\mathcal{V}, \prec)$ , the leaf cover of  $\mathcal{N}$ , denoted  $\text{leaf-cov}_{\mathcal{T}}(\mathcal{N})$ , is defined as:*

$$\bigcup_{v \in \mathcal{N}} \{w \in \text{leaves}(\mathcal{T}) \mid w \ll v \text{ or } w = v \in \text{leaves}(\mathcal{T})\}.$$

Based on the definition of a leaf cover, we put forward our goal to construct an optimal hierarchical conformal predictor  $h_{\beta, \mathcal{V}}^* : \mathcal{X} \times [0, 1) \rightarrow 2^{\mathcal{V}}$  that returns a set of nodes for any test pair  $(\mathbf{x}_t, y_t) \sim \mathcal{D}_t$ , such that:

$$h_{\beta, \mathcal{V}}^*(\mathbf{x}_t, \alpha) = \arg \min_{\mathcal{N} \subseteq \mathcal{V}} |\mathcal{N}| + \beta \left| \bigcup_{v \in \mathcal{N}} \text{leaf-cov}_{\mathcal{T}}(\{v\}) \right|$$

subject to  $\mathbb{P}(y_t \in \text{leaf-cov}_{\mathcal{T}}(\mathcal{N})) \geq 1 - \alpha. \quad (3)$

Here,  $\beta \in \mathbb{R}_+$  controls the trade-off between compactness and specificity, quantified as the number of covered leaves.

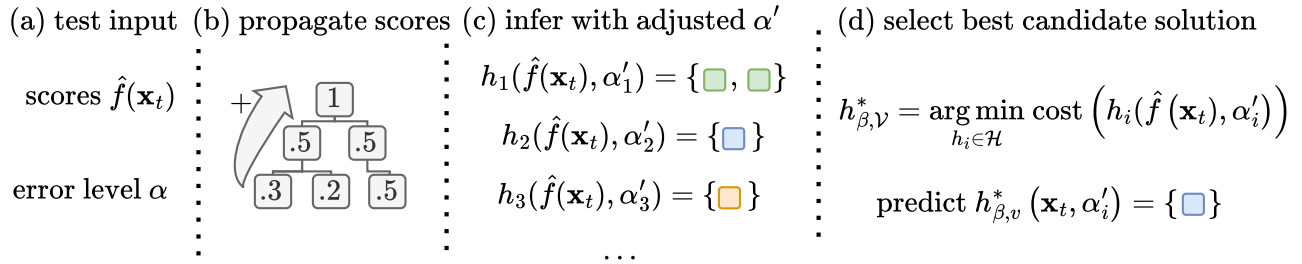


Figure 4: Visualization of HCC inference: (a) the prediction scores for a test input  $X_t$ , and for a desired error level  $\alpha$ , (b) the prediction scores are propagated, and (c) used to infer prediction sets using the calibrated classifiers obtained during training. Finally, (d) the prediction set that minimizes the cost, i.e. the objective in Equation (3) is selected.

A higher  $\beta$  prefers solutions that cover fewer leaves. Such solutions tend to include more nodes located higher in the hierarchy. The objective in minimization (3) expresses that the set  $\mathcal{N}$  must be compact and semantically meaningful, and the constraint guarantees that its leaf cover includes the ground-truth label with high probability.

At the heart of HCC is this constrained optimization problem, which formalizes the goal of producing valid and semantically coherent prediction sets under a given label hierarchy. However, solving this problem exactly is infeasible, as the number of candidate solutions grows combinatorially with the number of nodes in the DAG. To address this, HCC combines learning with efficient search strategies that exploit the hierarchical structure. Specifically, we first calibrate several conformal classifiers over a hierarchical label space, and then use these calibrated classifiers to guide an efficient inference-time procedure that approximates the optimal solution while maintaining coverage guarantees.

### Calibrating Hierarchical Classifiers

We consider the calibration of HCC in three phases, illustrated in Figure 3. Phase one consists of searching the search space. Instead of enumerating all node subsets, we restrict our attention to a much smaller family of subsets without affecting the optimality of the solution. Phase two comprises the propagation of the score and label. For every candidate subset, we propagate the labels and base classifier’s predicted scores from the leaf level upward, assigning to each internal node the logical OR of its leaf cover labels and the sum of the base classifier’s predictions. Finally, in phase three, we calibrate a conformal predictor on each subset with the propagated labels and the propagated base classifier scores. The collection of calibrated predictors constitutes our model family:

$$\mathcal{H} = \{h_S : S \subseteq \mathcal{V}\}.$$

We now elaborate on these three steps.

**Search-Space Pruning** The objective in equation (3) involves a minimization over all subsets  $\mathcal{S} \subseteq \mathcal{V}$ , which is of size  $2^{|\mathcal{V}|}$  and computationally infeasible for all but the smallest hierarchies. To address this, we propose an effective pruning of the search space based on two structural insights about the hierarchy. Specifically, we restrict our search to subsets of nodes that (i) collectively cover all leaves in the

hierarchy  $\mathcal{Y}$ , and (ii) do not include any ancestor–descendant pairs. We present these two notions in the following definition of *non-overlapping leaf covers*, and then show why these two desiderata are essential for efficient search.

**Definition 5** (NOL-cover). *A subset  $\mathcal{S} \subseteq \mathcal{V}$  is called a non-overlapping leaf cover (NOL-cover) if:*

1. **Leaf coverage** all leaves are covered by at least one node in  $\mathcal{S}$  via their descendants:  $\text{leaf-cov}_{\mathcal{T}}(\mathcal{S}) = \mathcal{Y}$ , and
2. **Ancestral independence** no two nodes in  $\mathcal{S}$  are related by an ancestor-descendant relationship:

$$\forall u, v \in \mathcal{S}, u \neq v \Rightarrow \neg(u \ll v) \wedge \neg(v \ll u).$$

For example, consider the running illustration in Figure 2. The set  $\{\text{breakfast}, \text{sandwich}\}$  fails to satisfy the leaf coverage requirement and therefore is not a valid NOL-cover. It could be extended to an NOL-cover by extending it with either  $\{\text{salad}\}$  or  $\{\text{Greek salad}, \text{Caesar salad}\}$ , but not both simultaneously, as this would violate the ancestral independence requirement.

We show that every conformal predictor optimal to problem (3) must be trained on a set that satisfies the leaf coverage requirement, since it would violate the probabilistic coverage requirement otherwise. All proofs are in the appendix.

**Proposition 1** (Necessity of leaf-coverage). *Any solution  $h_{\cdot, \mathcal{S}}$  feasible to Equation (3) must cover all leaves in  $\mathcal{Y}$ ; that is,  $\text{leaf-cov}_{\mathcal{T}}(\mathcal{S}) = \mathcal{Y}$ .*

We additionally show that the ancestral independence requirement excludes solutions that are suboptimal to (3).

**Proposition 2** (Sufficiency of ancestral independence). *Any solution to problem (3) is necessarily ancestral independent.*

These propositions suggest that it suffices to restrict the search space to NOL-covers only, thereby substantially reducing the search space in practice. The particular size of the reduction depends on the DAG, and we therefore characterize the reduction by considering the class of perfect binary trees of depth  $d$  for illustrative purposes. A naive search on all possible subsets of any such tree considers  $2^{2^d}$  hypotheses, which is reduced to  $\sim 2^{d-1}$  by considering only NOL-covers. In practice, multiple ancestry in DAGs, higher branching factors, and imbalance may further increase the

reduction. Thus, we greatly restrict the search space  $\mathcal{H}$  to the NOL-covers:

$$\mathcal{H} := \{h_S | S \in \text{NOL-covers}\}$$

to prune structurally redundant and invalid solutions.

**Propagating Scores and Labels** Each conformal classifier in  $\mathcal{H}$  is calibrated with respect to a specific subset of nodes in the DAG, including internal nodes. However, the classification scores  $\hat{f}$  and the ground-truth labels are available only for leaves. To enable calibration at arbitrary nodes, the classifier scores must be propagated upward. To do so, we sum the scores of all descendant leaves for each node and mark all ancestors of the true leaf as the ground truth label. This propagation ensures that every node in the DAG is associated with a predicted classification score and ground-truth label for each instance.

**Definition 6** (Propagated score). *For any node  $v \in \mathcal{V}$  the propagated score of  $v$  is defined as:*

$$\hat{g}(\mathbf{x})_v := \sum_{w \in \text{leaf-cov}_{\mathcal{T}}(\{v\})} \hat{f}(\mathbf{x})_w,$$

*i.e., the sum of the predicted scores of all leaf descendants of  $v$ , according to the base classifier  $\hat{f}$ .*

**Definition 7** (Propagated label). *For any input-label pair  $(\mathbf{x}_i, y_i)$ , the propagated ground-truth set for that instance  $i$  is defined as  $\mathcal{Y}'_i := \{v \in \mathcal{V} \mid y_i \in \text{leaf-cov}_{\mathcal{T}}(\{v\})\}$ , i.e., all ancestors of an instance’s ground-truth leaf node form its hierarchical ground-truth labels.*

If the hierarchy  $\mathcal{T}$  is a tree, then there is at most one ground-truth node per NOL-cover for each test instance. However, in the more general case where  $\mathcal{T}$  is a DAG but not a tree, multiple nodes in a NOL-cover may be in an instance’s ground-truth label set. Consequently, the CP task for a NOL-cover requires procedures tailored to the multi-label setting.

In multi-label classification, the ground truth labels can be represented by a vector indicating which labels are relevant. We here define such a ground-truth per NOL-cover, i.e., for a NOL-cover of size  $l$ , we define an associated label indicator vector  $\mathbf{y}_i \in \{0, 1\}^l$  where  $\mathbf{y}_{i,j} = 1$  if class  $j \in \mathcal{Y}'_i$  is relevant for example  $i$  and 0 otherwise. We provide details of the calibration and inference mechanisms for this setting below.

**Calibration** During calibration, a conformal predictor is constructed for each NOL-cover in the search space. Each predictor is then calibrated using aggregated scores and ground-truth labels as detailed previously. The calibration procedure follows the general split-CP process of estimating a quantile  $\hat{q}$  on a calibration set of conformity scores. In particular, in cases where  $\mathcal{T}$  is a tree, any preferred CP approach can be used. However, for the more general case where  $\mathcal{T}$  is a DAG, the calibration problem is more challenging due to the multi-label nature of the problem. We propose a novel conformity score function to address this challenge.

The function is based on the insight that multiple true labels correspond to a single ground-truth leaf, and that it suffices to include only one such label to satisfy the coverage

Table 1: Overview of data sets and models.

	dbp	img	gtz
$n$	56,000	10,000	1,000
# labels	14	1000	10
modality	text	image	audio
classifier	BERT	ResNet-152	XGBoost
accuracy	0.99	0.79	0.63
# nodes	25	1860	15
# leaves	14	1000	10
depth	6	17	3

condition in (3). We formalize this insight in a conformity score inspired by Sadinle, Lei, and Wasserman (2019):

$$s(\mathbf{x}_i, \mathbf{y}_i, \mathcal{S}) = \hat{g}(\mathbf{x}_i)_{v'_i} \quad (4)$$

where  $v'_i \in \mathcal{S}$  is the label with the highest classifier score:

$$v'_i := \arg \max_{j: \mathbf{y}_{i,j}=1} \hat{g}(\mathbf{x}_i)_j. \quad (5)$$

We note that this score trivially reduces to the selection of the prediction score for the ground truth label in the single-label setting. Therefore,  $s$  can be seen as a generalization of the score proposed by Sadinle, Lei, and Wasserman (2019) to a setting with hierarchically derived labels and scores  $\hat{g}$ .

We now show that the conformity score in (4) produces prediction sets with coverage guarantees over the hierarchy. In particular, it ensures that for any test instance  $\mathbf{x}_t$  and any allowed error rate  $\alpha \in [0, 1)$ , the probability that its ground truth leaf label  $y_t$  is a descendant of one of the nodes included in the prediction set is  $\geq 1 - \alpha$ .

**Theorem 1** (Hierarchical Coverage Guarantee). *Let  $\mathcal{S} \subseteq \mathcal{V}$  be a NOL-cover,  $(\mathbf{x}_t, y_t) \sim \mathcal{D}_t$  be an exchangeable test instance,  $\mathbf{y}_t$  the hierarchical ground truth label indicator for  $\mathcal{S}$  and  $y_t$ . Construct a prediction set as follows using the conformity score function  $s$  from Equation (4):*

$$C(\mathbf{x}_t) := \{v \in \mathcal{V} \mid s(\mathbf{x}_t, \mathbf{y}_t, \mathcal{S}) \leq \hat{q}\},$$

*where  $\hat{q}$  is the empirical quantile  $\lceil (n_c + 1)(1 - \alpha) \rceil / n_c$  of the calibration conformity scores  $\{s(\mathbf{x}_i, \mathbf{y}_i, \mathcal{S})\}_{i=1}^{n_c}$ . Then, the prediction set satisfies the hierarchical coverage guarantee*

$$\mathbb{P}[y_t \in \text{leaf-cov}_{\mathcal{T}}(C(\mathbf{x}_t))] \geq 1 - \alpha, \forall \alpha \in [0, 1).$$

The conformity score function can be further adapted to handle scenarios such as adaptive calibration or large label sets, and the related coverage guarantee proofs can be adapted analogously (Angelopoulos et al. 2021; Ding et al. 2023).

## Inference with Dynamic Pruning

We now detail how the family of conformal predictors is used to produce a prediction for a test instance  $\mathbf{x}_t$  and a target error level  $\alpha \in [0, 1)$ . We follow a three-step procedure based on the base classifier output  $\hat{f}$  (Figure 4a). The resulting scores are propagated upward to compute the propagated scores  $\hat{g}(\mathbf{x}_t)$  for all nodes, analogously to the propagation

Table 2: Test set results (mean±SD). **Bold** indicates meeting coverage guarantee for ‘coverage’ column, and, for other columns, the best out of all methods empirically meeting the desired coverage guarantee.

dataset	$\beta$	$1 - \alpha$	method	coverage $\uparrow$	costs $\downarrow$	PS size $\downarrow$	# covered leaves $\downarrow$
dbp	.19	.9997	Standard CP	<b>.9998</b> $\pm$ .02	3.18 $\pm$ 2.62	2.67 $\pm$ 2.20	<b>2.67</b> $\pm$ 2.20
			LCA	<b>.9999</b> $\pm$ .01	2.20 $\pm$ 1.13	<b>1</b> $\pm$ 0.00	6.32 $\pm$ 5.94
			HCC (ours)	<b>.9999</b> $\pm$ .01	<b>2.07</b> $\pm$ 1.00	1.25 $\pm$ 0.55	4.3 $\pm$ 4.65
			w/o dynamic pruning	<b>.9999</b> $\pm$ .01	2.40 $\pm$ 1.08	1.22 $\pm$ 0.47	6.18 $\pm$ 5.61
			w/o correction	<b>.9997</b> $\pm$ .02	1.88 $\pm$ 0.85	1.22 $\pm$ 0.43	3.44 $\pm$ 3.69
			w/o conformity	<b>.9999</b> $\pm$ .01	2.11 $\pm$ 1.05	1.29 $\pm$ 0.63	4.36 $\pm$ 4.71
img	.04	.98	Standard CP	<b>.9807</b> $\pm$ .14	11.49 $\pm$ 20.49	11.04 $\pm$ 19.70	<b>11.04</b> $\pm$ 19.70
			LCA	<b>.9951</b> $\pm$ .07	14.79 $\pm$ 15.63	<b>1</b> $\pm$ 0.00	344.7 $\pm$ 390.64
			HCC (ours)	<b>.9846</b> $\pm$ .12	<b>8.09</b> $\pm$ 11.01	4.41 $\pm$ 6.54	92.12 $\pm$ 245.12
			w/o dynamic pruning	.9791 $\pm$ .14	15.9 $\pm$ 13.40	2.46 $\pm$ 1.94	336.04 $\pm$ 327.04
			w/o correction	.9630 $\pm$ .19	4.51 $\pm$ 4.76	2.02 $\pm$ 1.59	62.17 $\pm$ 107.35
			w/o conformity	.9497 $\pm$ .22	2.90 $\pm$ 3.43	2.57 $\pm$ 3.22	8.38 $\pm$ 25.92
gtz	.25	.9	Standard CP	<b>.9613</b> $\pm$ .19	2.73 $\pm$ 0.97	1.19 $\pm$ 0.39	6.17 $\pm$ 4.14
			LCA	.9812 $\pm$ .14	2.86 $\pm$ 1.01	1 $\pm$ 0.00	7.45 $\pm$ 4.02
			HCC (ours)	<b>.9637</b> $\pm$ .19	2.76 $\pm$ 0.98	1.11 $\pm$ 0.32	6.57 $\pm$ 4.24
			w/o dynamic pruning	<b>1</b> $\pm$ .00	3.41 $\pm$ 0.35	1.07 $\pm$ 0.26	9.35 $\pm$ 2.11
			w/o correction	<b>.9275</b> $\pm$ .26	2.47 $\pm$ 0.94	1.33 $\pm$ 0.47	<b>4.56</b> $\pm$ 3.75
			w/o conformity	<b>.9575</b> $\pm$ .20	<b>2.67</b> $\pm$ 0.97	1.18 $\pm$ 0.38	5.97 $\pm$ 4.22

of the scores in the calibration phase (Figure 4b). Each calibrated conformal predictor  $h_i \in \mathcal{H}$  is then evaluated on these scores with an adjusted  $\alpha$ , and produces a candidate prediction set (Figure 4c). The candidate that minimizes the cost term in (3) is selected (Figure 4d) to effectively form  $h_{\beta, \gamma}^*$  for that instance  $\mathbf{x}_t$ .

Since inference involves evaluating multiple conformal classifiers in parallel, we need to correct the user-selected  $\alpha$  to account for multiple comparisons. In particular, when running CP for each of the  $m$  selected NOL-covers for an instance, we use the well-understood and conservative Bonferroni correction  $\alpha' = \alpha/m$  to maintain coverage guarantees (Sedgwick 2012). This, however, may lead to large corrections and large prediction sets when the number of NOL-covers is large.

We therefore propose to limit the search further during inference. In doing so, we first observe that the set of candidate NOL-covers includes both the set of all leaves  $\mathcal{V}$  and all sets containing the lowest common ancestor of the prediction set generated by the conformal classifier associated with the leaves. We therefore dynamically prune all solutions associated with NOL-covers that contain an ancestor of an LCA of these leaves from the search, and consider all solutions that include an LCA as equivalent to further reduce the search dynamically during inference.

## Experiments

**Datasets** To rigorously evaluate our approach across modalities and classification paradigms, we curated and utilized *three distinct benchmark datasets*, each paired with a structured taxonomy and a representative base classifier. These datasets—*spanning text, image, and audio modalities*—are as follows:

- **DBpedia14 (dbp)** – A *text classification* task built on Wikipedia abstracts, using a subset of the DBpedia taxonomy. We employed a BERT-based classifier (Zhang, Zhao, and LeCun 2015). The labels were mapped to their ancestors using the DBpedia ontology (Mendes, Jakob, and Bizer 2012).
- **ImageNet1K (img)** – An *image dataset* with 1,000 object categories organized under the deep and rich WordNet hierarchy (Russakovsky et al. 2015; Miller 1995). We used a ResNet-style classifier (He et al. 2016) to evaluate our method under a challenging visual taxonomy.
- **GTZAN Genre Collection (gtz)** – An *audio classification* dataset containing 1,000 music clips across 10 genres, structured into a hierarchical taxonomy as introduced by Sturm (2012). This dataset enables testing our method in the acoustic domain.

The datasets are summarized in Table 1. For all datasets, we used a fixed 80/20 calibration/test split. The release of these datasets—along with their taxonomies and model outputs—paves the way for future research on conformal prediction in hierarchical settings.

Parameters of the approach were set as follows:  $\alpha$  was set based on the hardness of the classification task, i.e., inversely proportional to the accuracy of the classifier.  $\beta$  was established on the basis of the median number of covered leaves for every node in the DAG. Specifically, this value was set to

$$\beta := \left( \text{median}[\{\text{leaf-cov}_{\mathcal{T}}(\{v\}) \mid v \notin \text{leaves}(\mathcal{T})\}]_{v \in \mathcal{V}} \right)^{-1} \quad (6)$$

for the main results. This parameter was also varied to assess its impact on the nominal prediction set size and the number of covered leaves.

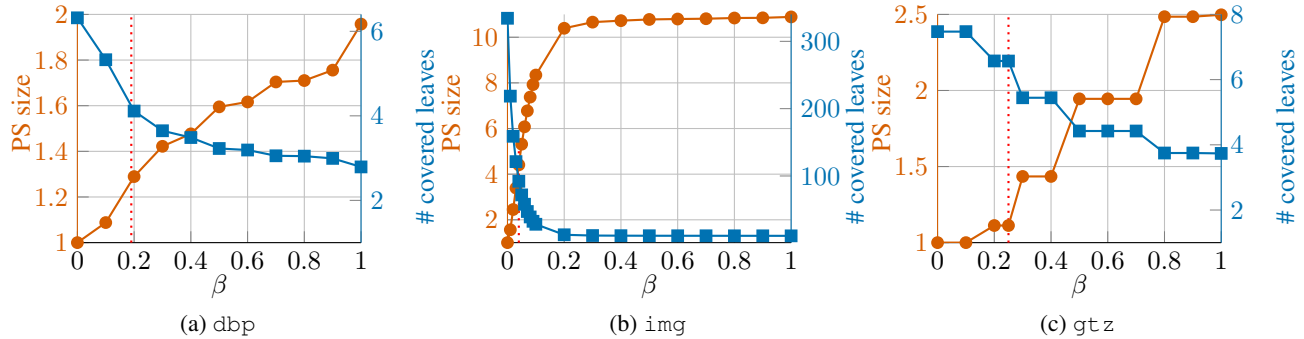


Figure 5: Prediction set sizes and number of covered leaves for varying  $\beta$ , dotted red lines indicate  $\beta$  in Table 3.

**Baselines and Ablations** We compare HCC against several baselines. **Standard CP** predicts on the leaves  $\mathcal{Y}$  only and **LCA** forms a prediction set by returning the lowest common ancestor of a prediction set created by standard CP. We furthermore include several ablations. We ablate **dynamic pruning** which requires a single Bonferroni correction across the entire test set, we ablate Bonferroni **correction** altogether by using the original  $\alpha$ , and we ablate the hierarchical **conformity** score in (4) by replacing it with the multi-label recall loss within the conformal risk control framework by Angelopoulos et al. (2024). We additionally include a direct comparison with conformal structured prediction Zhang, Li, and Bastani (2025) on a different  $\alpha$  value in the supplementary material as this approach produce results for the input and  $\alpha$ -values in our main experiment.

**Results** We list our main results in Table 3. We observe that the coverage requirement of  $1 - \alpha$  is met for all baselines but not for all ablations, and that HCC produces solutions with the lowest (dbp, img) or comparable to the lowest cost (gtz). Furthermore, we note in the column *PS size*, which denotes the average number of elements in the prediction set, that HCC produces significantly smaller prediction sets on average for all data sets. Next, in the column *# covered leaves* we see that the nominally smaller prediction sets produced by HCC come at a moderate cost to the total number of covered leaves. The cost refers to the compactness and semantic clarity of the set (c.f. Equation (3)). Furthermore, Figure 5 shows how HCC allows a fine-grained control of the prediction set size against the number of covered leaves.

**User Study** We also assess the utility of HCC with a moderately sized user study, based on the preference of four annotators for HCC or standard CP in 500 random samples of the dbp and img datasets. The interannotation agreement was fair to moderate with Fleiss’s Kappa values of 0.47 for dbp and 0.53 for img. The results of a binomial test indicate a significant preference for HCC over standard CP in approximately 57% and 71% of cases, respectively, for dbp and img, highlighting HCC’s practical utility.

## Discussion

This work is, to the best of our knowledge, the first to propose an efficient search for the problem of conformal pre-

diction over a hierarchical label space that allows the trading off nominal prediction set size and specificity, which is here quantified as the number of covered leaves, with coverage guarantees. While our results are promising, we believe that there is ample room to improve and extend our approach to various settings. For example, our moderately scaled user study encourages a larger user study on a realistic use case (den Hengst et al. 2024). Here, we can also consider optimizing for  $\beta$  based on user preferences.

Additionally, our approach itself can be improved in various ways. Firstly, we apply the Bonferroni correction to the user-specified  $\alpha$  levels to address the multiple comparison problem, but this correction is known to be overly conservative, and more advanced correction methods from sequential testing can be applied (Holm 1979) if the expected costs associated with each calibrated predictor in  $\mathcal{H}$  can be ordered meaningfully. We expect that this would change the results in favor of our approach.

Moreover, we believe that there is room for improvement by further reducing the search during inference, as this would reduce the number of comparisons and hence the correction applied to  $\alpha$ . There are various directions here. One example direction involves using the hierarchy to assess which conformal predictors are likely to produce similar sets, and another direction involves selecting the predictors based on the distribution of scores over classification nodes with a similar aim. All of the suggested improvements are expected to change the results in favor of our approach.

## Conclusion

In this paper, we argued the importance of background knowledge in creating informative, concise, and connected conformal prediction sets. We then formally introduce the task of hierarchical conformal classification, in which the target labels for classification are organized in a hierarchy. We propose an initial solution based on a search over the space of relevant conformal predictors for the given hierarchy and evaluate it in simulation and in a user study based on using three datasets. Our results indicate that the usage of hierarchical information can lead to better prediction sets in both types of evaluation, and we find that annotators significantly prefer our approach in our user study.

## Acknowledgments

We kindly thank our reviewers for their time and their useful comments. We thank Xander Wilcke for the useful discussions during the initial phases of this project. This research was partially funded by the Hybrid Intelligence Centre, a 10-year programme supported by the Dutch Ministry of Education, Culture and Science through the Netherlands Organisation for Scientific Research (NWO), under grant number 024.004.022.

## References

- Angelopoulos, A. N.; Bates, S.; Candès, E. J.; Jordan, M. I.; and Lei, L. 2025. Learn then test: Calibrating predictive algorithms to achieve risk control. *The Annals of Applied Statistics*, 19(2): 1641–1662.
- Angelopoulos, A. N.; Bates, S.; Fisch, A.; Lei, L.; and Schuster, T. 2024. Conformal Risk Control. In *The Twelfth International Conference on Learning Representations*.
- Angelopoulos, A. N.; Bates, S.; Jordan, M.; and Malik, J. 2021. Uncertainty Sets for Image Classifiers using Conformal Prediction. In *The Ninth International Conference on Learning Representations*.
- Angelopoulos, A. N.; Bates, S.; et al. 2023. Conformal prediction: A gentle introduction. *Foundations and Trends® in Machine Learning*, 16(4): 494–591.
- Bennett, M. 2013. The financial industry business ontology: Best practice for big data. *Journal of Banking Regulation*, 14(3): 255–268.
- Cauchois, M.; Gupta, S.; and Duchi, J. C. 2021. Knowing what you know: valid and validated confidence sets in multi-class and multilabel prediction. *Journal of machine learning research*, 22(81): 1–42.
- den Hengst, F.; Wolter, R.; Altmeyer, P.; and Kaygan, A. 2024. Conformal Intent Classification and Clarification for Fast and Accurate Intent Recognition. In Duh, K.; Gomez, H.; and Bethard, S., eds., *Findings of the Association for Computational Linguistics: NAACL 2024*, 2412–2432. Mexico City, Mexico: Association for Computational Linguistics.
- Ding, T.; Angelopoulos, A.; Bates, S.; Jordan, M.; and Tibshirani, R. J. 2023. Class-conditional conformal prediction with many classes. *Advances in neural information processing systems*, 36: 64555–64576.
- He, K.; Zhang, X.; Ren, S.; and Sun, J. 2016. Deep residual learning for image recognition. In *Proceedings of the IEEE conference on computer vision and pattern recognition*, 770–778.
- Holm, S. 1979. A simple sequentially rejective multiple test procedure. *Scandinavian journal of statistics*, 65–70.
- Lambrou, A.; and Papadopoulos, H. 2016. Binary relevance multi-label conformal predictor. In *Conformal and Probabilistic Prediction with Applications: 5th International Symposium, COPA 2016, Madrid, Spain, April 20-22, 2016, Proceedings 5*, 90–104. Springer.
- Maltoudoglou, L.; Paisios, A.; Lenc, L.; Martínek, J.; Král, P.; and Papadopoulos, H. 2022. Well-calibrated confidence measures for multi-label text classification with a large number of labels. *Pattern Recognition*, 122: 108271.
- Mendes, P. N.; Jakob, M.; and Bizer, C. 2012. *DBpedia: A multilingual cross-domain knowledge base*. European Language Resources Association (ELRA).
- Miller, G. A. 1995. WordNet: a lexical database for English. *Communications of the ACM*, 38(11): 39–41.
- Mortier, T.; Hüllermeier, E.; Dembczyński, K.; and Waegeman, W. 2022. Set-valued prediction in hierarchical classification with constrained representation complexity. In *Uncertainty in Artificial Intelligence*, 1392–1401. PMLR.
- Mortier, T.; Javanmardi, A.; Sale, Y.; Hüllermeier, E.; and Waegeman, W. 2025. Conformal Prediction in Hierarchical Classification. *arXiv preprint arXiv:2501.19038*.
- Paisios, A.; Lenc, L.; Martínek, J.; Král, P.; and Papadopoulos, H. 2019. A Deep Neural Network Conformal Predictor for Multi-label Text Classification. In Gammerman, A.; Vovk, V.; Luo, Z.; and Smirnov, E., eds., *Proceedings of the Eighth Symposium on Conformal and Probabilistic Prediction and Applications*, volume 105 of *Proceedings of Machine Learning Research*, 228–245. PMLR.
- Papadopoulos, H. 2014. A cross-conformal predictor for multi-label classification. In *Artificial Intelligence Applications and Innovations: AIAI 2014*, 241–250. Springer.
- Russakovsky, O.; Deng, J.; Su, H.; Krause, J.; Satheesh, S.; Ma, S.; Huang, Z.; Karpathy, A.; Khosla, A.; Bernstein, M.; et al. 2015. Imagenet large scale visual recognition challenge. *International journal of computer vision*, 115: 211–252.
- Sadinle, M.; Lei, J.; and Wasserman, L. 2019. Least ambiguous set-valued classifiers with bounded error levels. *Journal of the American Statistical Association*, 114(525): 223–234.
- Sedgwick, P. 2012. Multiple significance tests: the Bonferroni correction. *Bmj*, 344.
- Sturm, B. L. 2012. An analysis of the GTZAN music genre dataset. In *Proceedings of the second international ACM workshop on Music information retrieval with user-centered and multimodal strategies*, 7–12.
- Tyagi, C.; and Guo, W. 2023. Multi-label classification under uncertainty: a tree-based conformal prediction approach. In *Conformal and Probabilistic Prediction with Applications*, 488–512. PMLR.
- Vovk, V.; Gammerman, A.; and Shafer, G. 2005. *Algorithmic learning in a random world*, volume 29. Springer.
- Wang, H.; Liu, X.; Lv, B.; Yang, F.; and Hong, Y. 2014. Reliable multi-label learning via conformal predictor and random forest for syndrome differentiation of chronic fatigue in traditional Chinese medicine. *PloS one*, 9(6): e99565.
- Wieslander, H.; Harrison, P. J.; Skogberg, G.; Jackson, S.; Fridén, M.; Karlsson, J.; Spjuth, O.; and Wählby, C. 2020. Deep learning with conformal prediction for hierarchical analysis of large-scale whole-slide tissue images. *IEEE journal of biomedical and health informatics*, 25(2): 371–380.
- Zesch, T.; and Gurevych, I. 2007. Analysis of the Wikipedia category graph for NLP applications. In *Proceedings of the*

*Second Workshop on TextGraphs: Graph-Based Algorithms for Natural Language Processing*, 1–8.

Zhang, B.; Li, S.; and Bastani, O. 2025. Conformal Structured Prediction. In *The Thirteenth International Conference on Learning Representations*.

Zhang, X.; Zhao, J.; and LeCun, Y. 2015. Character-level convolutional networks for text classification. *Advances in neural information processing systems*, 28.

## Appendix A: Proofs

We here provide proofs for all theoretical results:

*Proposition (1)* (Necessity of leaf-coverage). Any solution  $h_{\cdot, \mathcal{S}}$  feasible to Equation (3) must cover all leaves in  $\mathcal{Y}$ ; that is,  $\text{leaf-cov}_{\mathcal{T}}(\mathcal{S}) = \mathcal{Y}$ .

*Proof to Proposition (1)*. Suppose, for contradiction, that there exists a subset  $\mathcal{M} \subseteq \mathcal{V}$  such that  $\text{leaf-cov}_{\mathcal{T}}(\mathcal{M}) \subset \mathcal{Y}$ . Then, there exists at least one leaf  $y^* \in \mathcal{Y}$  such that  $y^* \notin \text{leaf-cov}_{\mathcal{T}}(\mathcal{M})$ . Assume the data distribution  $\mathcal{D}$  satisfies  $\mathbb{P}(y = y^*) > 0$ , which must hold unless  $y^*$  is excluded from  $\mathcal{Y}$  altogether.

Since  $y^* \notin \text{leaf-cov}_{\mathcal{T}}(\mathcal{M})$ , we have  $\mathbb{P}(y = y^*, y \in \text{leaf-cov}_{\mathcal{T}}(\mathcal{M})) = 0$ . Therefore,

$$\mathbb{P}(y \in \text{leaf-cov}_{\mathcal{T}}(\mathcal{M})) \leq 1 - \mathbb{P}(y = y^*).$$

As a result, for any  $\alpha \in [0, \mathbb{P}(y = y^*)]$ , we have

$$\mathbb{P}(y \in \text{leaf-cov}_{\mathcal{T}}(\mathcal{M})) < 1 - \alpha$$

which contradicts with the requirement in Equation (3). □

*Proposition (2)* (Sufficiency of ancestral independence). Any solution to problem (3) is necessarily ancestral independent.

*Proof to Proposition (2)*. Let  $\mathcal{N}^* \subseteq \mathcal{V}$  be any feasible solution to the objective in Equation (3) and let  $\mathcal{S}_{\text{NOL}}$  denote the set of all non-overlapping leaf covers following Definition 5. If  $\mathcal{N}^* \in \mathcal{S}_{\text{NOL}}$ , we are done. Otherwise, we show how to construct a set  $\mathcal{S} \in \mathcal{S}_{\text{NOL}}$  with lower or equal cost.

We construct  $\mathcal{S}$  from  $\mathcal{N}^*$  by removing any node  $u \in \mathcal{N}^*$  that is a proper ancestor or descendant of another node  $v \in \mathcal{N}^*$ . We continue this process until no more ancestors are present.

The resulting set  $\mathcal{S} \subseteq \mathcal{V}$  now satisfies by construction:

$$\forall u, v \in \mathcal{S}, u \neq v \Rightarrow \neg(u \ll v) \wedge \neg(v \ll u).$$

and both  $|\mathcal{S}| \leq |\mathcal{N}^*|$  and  $|\bigcup_{v \in \mathcal{S}} \text{leaf-cov}_{\mathcal{T}}(v)| \leq |\bigcup_{v \in \mathcal{N}^*} \text{leaf-cov}_{\mathcal{T}}(v)|$ , since redundant coverage was eliminated.

Therefore,  $\mathcal{S} \in \mathcal{S}_{\text{NOL}}$  is a feasible solution with objective value no greater than that of  $\mathcal{N}^*$ . This holds for all feasible  $\mathcal{N}^*$ , so the search can be restricted to the conformal classifiers calibrated on the NOL-cover set without incurring additional cost. □

*Theorem (1)* (Hierarchical Coverage Guarantee). Let  $\mathcal{S} \subseteq \mathcal{V}$  be a NOL-cover,  $(\mathbf{x}_t, y_t) \sim \mathcal{D}_t$  be an exchangeable test instance,  $\mathbf{y}_t$  the hierarchical ground truth label indicator for  $\mathcal{S}$  and  $y_t$ . Construct a prediction set as follows using the conformity score function  $s$  from Equation (4):

$$C(\mathbf{x}_t) := \{v \in \mathcal{V} \mid s(\mathbf{x}_t, \mathbf{y}_t, \mathcal{S}) \leq \hat{q}\},$$

where  $\hat{q}$  is the empirical quantile  $\lceil (n_c + 1)(1 - \alpha)/n_c \rceil$  of the calibration conformity scores  $\{s(\mathbf{x}_i, \mathbf{y}_i, \mathcal{S})\}_{i=1}^{n_c}$ . Then, the prediction set satisfies the hierarchical coverage guarantee

$$\mathbb{P}[y_t \in \text{leaf-cov}_{\mathcal{T}}(C(\mathbf{x}_t))] \geq 1 - \alpha, \forall \alpha \in [0, 1].$$

*Proof to Theorem (1)*. By construction, the conformity score  $s(\mathbf{x}_i, \mathbf{y}_i, \mathcal{S})$  selects the node  $v' \in \mathcal{S} \cap \mathcal{Y}'$  in the NOL-cover  $\mathcal{S}$  with the highest classification score and assigns the score  $\hat{g}(\mathbf{x})_{v'}$ . Let  $s_i$  denote this score for some particular pair  $(\mathbf{x}_i, \mathbf{y}_i)$  and an arbitrary NOL-cover  $\mathcal{S}$ .

Given the exchangeability of the calibration examples and the test instance, the set of conformity scores  $\{s_1, \dots, s_{n_c}, s_t\}$  is also exchangeable. Therefore, the rank of  $s_t$  among these  $n_c + 1$  scores is uniformly distributed over  $\{1, \dots, n_c + 1\}$ .

It follows that:

$$\mathbb{P}[s_t \leq \hat{q}] \geq 1 - \alpha.$$

Now observe that:

$$s_t \leq \hat{q} \iff \hat{g}(\mathbf{x}_t)_{v'_t} \geq 1 - \hat{q} \iff v'_t \in C(\mathbf{x}_t),$$

where  $v'_t := \arg \max_{j \in \mathcal{S} \cap \mathcal{Y}'_t} \hat{g}(\mathbf{x}_t)_j$  is a node in the NOL-cover which has been labeled as ground truth.

By definition of the propagated label set, since  $y_t \in \text{leaf-cov}_{\mathcal{T}}(\{v'_t\})$ , and  $v'_t \in C(\mathbf{x}_t)$ , it follows that:

$$y_t \in \text{leaf-cov}_{\mathcal{T}}(C(\mathbf{x}_t)).$$

Therefore,

$$\mathbb{P}[y_t \in \text{leaf-cov}_{\mathcal{T}}(C(\mathbf{x}_t))] = \mathbb{P}[s_t \leq \hat{q}] \geq 1 - \alpha.$$

□

## Appendix B: Perfect Binary Search Space Analysis

A perfect binary tree is a balanced binary tree where all leaves reside at the same depth  $d$ . For any such tree, the total number of leaves is

$$|\mathcal{V}| = 2^d,$$

and hence the total naive search space size is

$$2^{|\mathcal{V}|} = 2^{2^d}.$$

The NOL-cover size can be inferred by defining the size recursively from the root down using the sequence  $C(d)$  as:

$$C(0) = 1$$

$$C(1) = 2$$

$$C(2) = 5$$

$$C(d) = C(d-1) + \frac{2^{d-1}(2^{d-1} + 1)}{2} + 1, \quad \text{for } d > 2$$

We can write  $C(d)$  as a summation for  $d > 2$ :

$$C(d) = C(2) + \sum_{k=3}^d \left( \frac{2^{k-1}(2^{k-1} + 1)}{2} + 1 \right)$$

And approximate at a marginal loss of accuracy:

$$C(d) \approx \sum_{k=3}^d (2^{2k-3} + 2^{k-2} + 1)$$

We approximate each component of the summation:

$$\sum_{k=3}^d 2^{2k-3} = 8 \sum_{j=0}^{d-3} 4^j = \frac{8}{3}(4^{d-2} - 1)$$

$$\sum_{k=3}^d 2^{k-2} = 2^{d-1} - 2, \quad \sum_{k=3}^d 1 = d - 2$$

Combining all:

$$C(d) \approx \frac{8}{3}(4^{d-2} - 1) + (2^{d-1} - 2) + (d - 2)$$

$$C(d) \approx \frac{8}{3} \cdot 4^{d-2} + 2^{d-1} + d - \frac{14}{3}$$

which has dominant term  $2^{d-1}$ .

## Appendix C: Search Space Construction

An algorithm for finding NOL-covers is shown in Alg. 1. It generates all valid NOL-covers in a top-down recursive way, starting from the set of root nodes in  $\mathcal{T}$  (ln 16-18), which is a NOL-cover by definition. The recurrence step involves first validating that the current candidate contains no overlapping nodes and has not already been added to the result (ln 2-4). The candidate is added to the result if it covers all leaves (ln 5-6). New candidates are formed by replacing each node in the set with its children, and these new candidates are then recurred upon (ln 7-12) until all NOL-covers are found.

While Alg. 1 needs to be run only once per taxonomy and can in practice be implemented efficiently using caching and parallel execution, some taxonomies may generate a large search space, resulting in long running times and large corrections to the allowed error  $\alpha$ . In this case, the limited search can be employed, based on the depths of taxonomy  $\mathcal{T}$  with maximum depth  $d$ , where a NOL-cover for each depth  $0, 1, \dots, d_i, \dots, d$  contains all nodes at that depth  $d_i$  and all leaves at a lower depth  $d_j \leq d_i$ .

---

Algorithm 1: Algorithm for finding all NOL-covers

---

**Input:** DAG  $\mathcal{T}$  with nodes  $\mathcal{V}$

**Output:** Non-overlapping leaf covers

```

1: procedure RECUR(candidate,  $\mathcal{T}$ , result)
2:   if ANCESTORS(candidate,  $\mathcal{T}$ ) or candidate  $\in$  result then
3:     return {invalid candidate}
4:   end if
5:   if cov $_T$ (candidate) = leaves( $\mathcal{T}$ ) then
6:     result.append(candidate) {add candidates}
7:     for all n  $\in$  candidate do
8:       new-candidate  $\leftarrow$  candidate.copy()
9:       new-candidate.remove(n) {replace by children}
10:      new-candidate.add(n.expand())
11:      call RECUR(new-candidate,  $\mathcal{T}$ , result)
12:    end for
13:  end if
14:  return
15: end procedure
16: noI-covers  $\leftarrow$  List()
17: candidate  $\leftarrow$  Set(root( $\mathcal{T}$ )) {initial candidate}
18: RECUR(candidate,  $\mathcal{T}$ , noI-covers) {start recursion}
19: return noI-covers

```

---

### Appendix D: Data and Taxonomies

We here list the distribution of nodes per level for all taxonomies and visualise the taxonomies for `dbp` and `gtz`. The full taxonomy for `img` is omitted due to size.

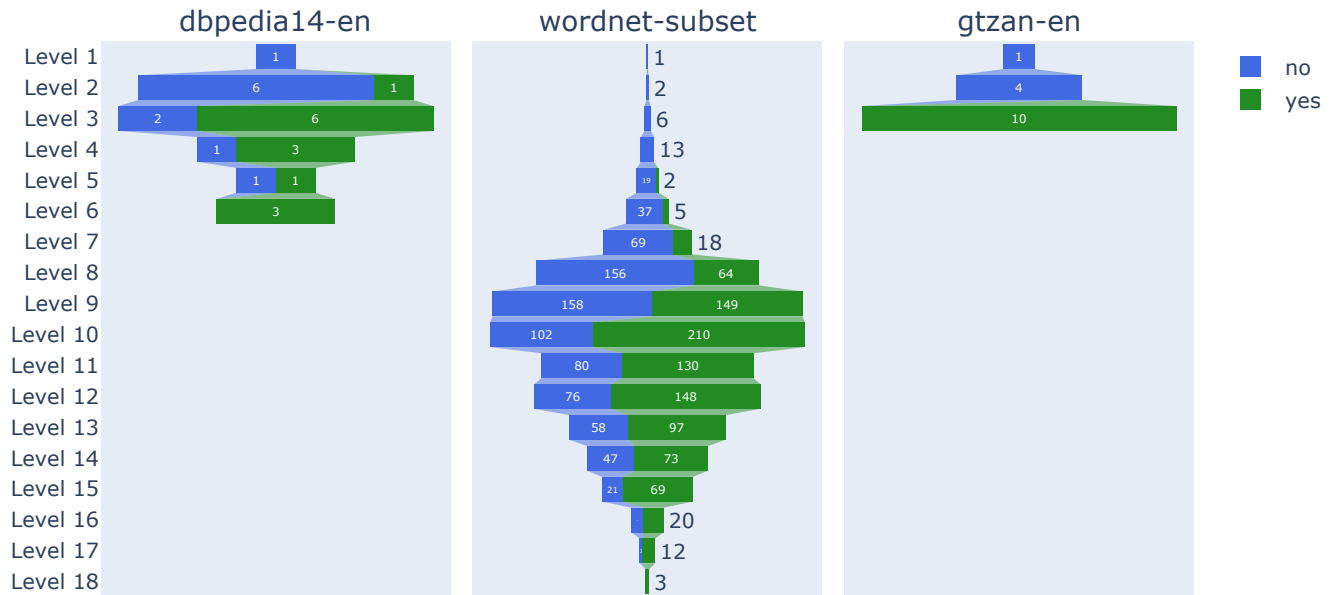


Figure 6: Number of nodes per level: `dbp` (left) and `wordnet-subset` (center), `gtz` (right). "yes" denotes the number of leaves, and "no" the number of internal nodes per level.

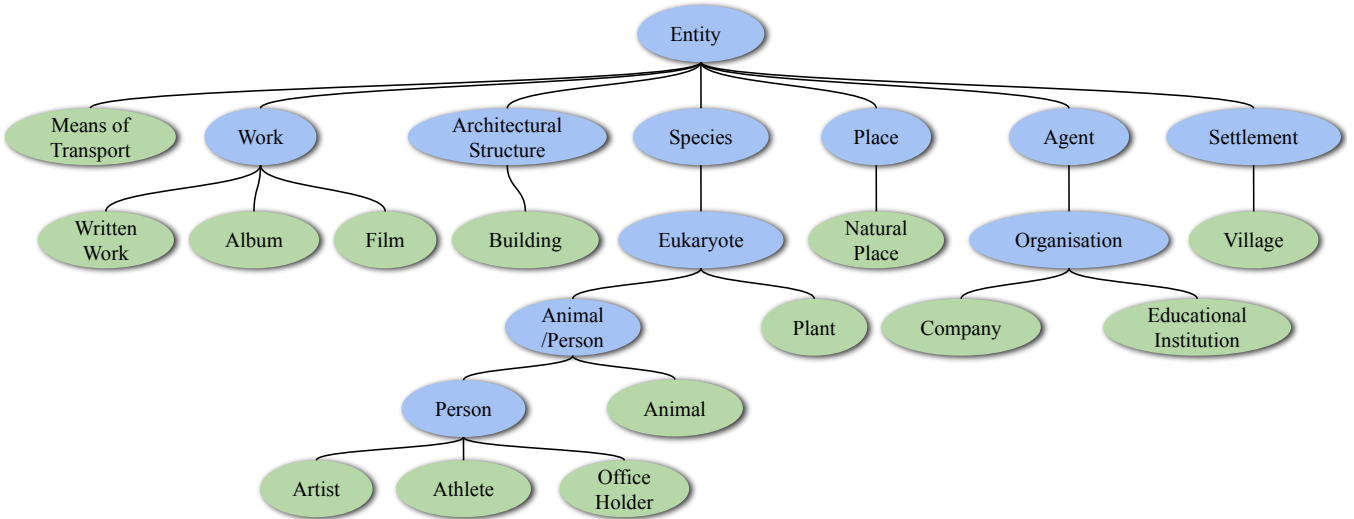


Figure 7: dbp taxonomy. Leaves are denoted in green and intermediate nodes in blue.

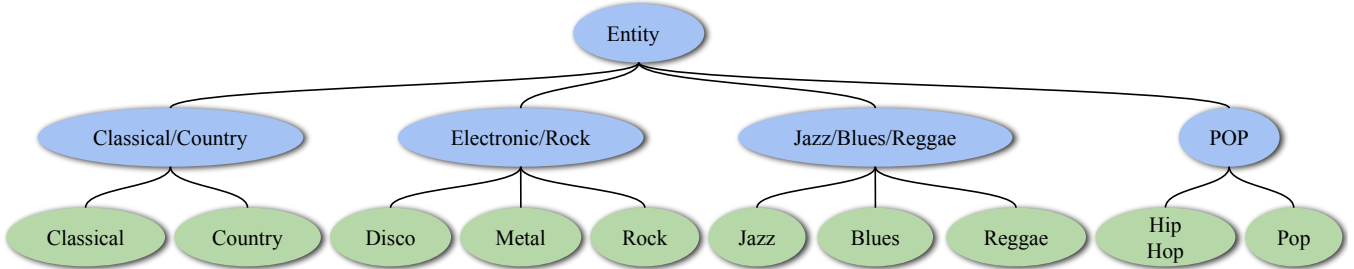


Figure 8: gtz taxonomy.

## Appendix E: Additional Results & Ablation Details

We compare our approach to Structured Conformal Prediction (SCP) by Zhang, Li, and Bastani (2025) on the ImageNet dataset, using prediction scores obtained with the same ResNet-152 base classifier on the same dataset with values  $M = [4, 8]$ . We use their implementation but substitute the commercial Gurobi solver with GLPK-MI. The approach failed to obtain results for the  $\alpha = 0.02$  that we established based on the performance of the base classifier. We therefore compare against this approach with  $\alpha = 0.1$ .

Table 3: Additional test set results (mean).

dataset	$\beta$	$1 - \alpha$	method	coverage $\uparrow$	costs $\downarrow$	PS size $\downarrow$	# covered leaves $\downarrow$
img	.04	.9	Standard CP	0.8982	1.82	1.75	1.75
			LCA	<b>0.9494</b>	5.58	<b>1</b>	114.59
			SCP $M = 4$	<b>0.9262</b>	2.78	1.64	21.27
			SCP $M = 8$	<b>0.9188</b>	2.50	2.13	10.54
			HCC (ours)	<b>0.9036</b>	<b>1.63</b>	1.49	<b>3.57</b>

An existing approach to multi-label conformal prediction can be employed, e.g., following the conformal risk-control framework by Angelopoulos et al. (2024). This approach controls the risk that some monotone loss  $L$  on any sample  $x_{n_c+1}$  not seen during calibration by a single hyperparameter  $\alpha$ :

$$\mathbb{E} [L_{n_c+1}(\hat{\lambda})] \leq \alpha. \quad (7)$$

and can be used with a recall loss

$$L_t^R = \frac{\sum_{i \in C(\mathbf{x}_t)} \mathbf{y}_{t,i}}{\sum \mathbf{y}_t} \quad (8)$$

where  $\mathbf{y}_t$  is a ground-truth indicator constructed as described in the main body and  $C(\mathbf{x}_t)$  is a prediction set.

## Appendix F: User Study Details

We assessed our approach using a moderately scaled user study, in which the authors provided their preference on 500 random samples with differing prediction sets for the `dbp` and `img` datasets. Annotators were asked to indicate their preference for one result over the other or to indicate no preference. The Fleiss’ Kappa values for inter-annotator agreement were 0.47 and 0.33 for these datasets, respectively. This indicates a fair (`dbp`) to moderate (`img`) level of agreement.

Table 4 shows the annotation and majority distribution across the labels *HCC*, *standard CP*, and *no preference*, for both `dbp` and `img`. Overall, HCC was favoured by annotators, both in annotation numbers (52.4% and 57.9% for `dbp` and `img`) and in majority distribution numbers (50.4% for both).

We applied the binomial test to evaluate whether the number of annotators who preferred hierarchical over vanilla differed significantly from what would be expected by chance ( $p = 0.05$ ). The binomial tests indicate a significant preference for hierarchical over vanilla for both datasets, with test statistics of 0.57 for `dbp` and 0.71 for `img`, and p-values of  $3.4 \times 10^{-5}$  and  $2.4 \times 10^{-33}$ . This means that in approximately 57% and 71% of cases, respectively, annotators preferred hierarchical over vanilla, which is significantly higher than expected by chance.

User preferences varied by domain and task. In `dbp`, differing taxonomies and HCC’s abstract outputs made prediction sets less helpful, while standard CP was more precise at the cost of larger sets. In `img`, users preferred standard CP for small sets and HCC when unsure or faced with fine-grained categories. Abstract labels (e.g., “object”) were generally unhelpful. Preferences often depended on whether the task called for broad recognition or fine-grained detail, suggesting future evaluations should consider task context. Moreover, in `img`, several samples consist of multiple objects in one image, while the ground truth label is only one, i.e., each item has a single label rather than multiple labels, and the classifier is trained on multiclass classification rather than multilabel classification. In such cases, standard CP often predicts a large set of labels while HCC may prefer ancestors, which can usually lead to abstract outputs such as “object” or “artifact”. An in-depth study of the impact of such samples on different CP models can be a direction for future research.

Table 4: Annotation and majority distribution across the preferences *HCC* (ours), *Standard CP* and *No Preference*. The best results are shown in **bold**.

Metric		Preference		
		HCC	Standard CP	No Preference
<code>dbp</code>	Annotation distribution (#)	523	401	74
	Annotation distribution (%)	52.4	40.2	7.4
	Majority distribution (#)	126	90	12
	Majority distribution (%)	50.4	36.0	4.8
<code>img</code>	Annotation distribution (#)	577	239	180
	Annotation distribution (%)	57.9	24.0	18.1
	Majority distribution (#)	126	35	46
	Majority distribution (%)	50.4	14.0	18.4

## Appendix G: Additional Related work

In this section, we discuss additional studies on conformal prediction that leverage some structure over the prediction target and compare these approaches to HCC.

In the context of multilabel classification problems, conformal prediction approaches include Binary Relevance Multi-Label Conformal Predictor (BR-MLCP) (Lambrou and Papadopoulos 2016), the instance-based method (Wang et al. 2014), and Power Set Multi-Label Conformal Predictor (PS-MLCP1) (Papadopoulos 2014). PS-MLCP1 has been applied in text classification tasks (Paisios et al. 2019), and an extension of PS-MLCP1 effectively manages large labels (Maltoudoglou et al. 2022). BR-MLCP uses a one-against-all approach to break down a multilabel dataset into multiple single-label binary classification tasks. However, this approach fails to consider the dependencies between labels. On the other hand, PS-MLCP1 takes label dependencies into account but fails to address missing label information and faces computational issues when dealing with large labels. Cauchois, Gupta, and Duchi (2021) established a tree-structured technique to consider the interaction between the labels. Tyagi and Guo (2023) proposed a tree-based method for multilabel classification problems using conformal prediction and multiple testing.

## Appendix H: Compute Infrastructure

All experiments were conducted on a machine equipped with an Apple M2 Pro chip (10-core CPU, 16-core GPU) and 32 GB of unified memory. The operating system used was macOS Ventura 13.5. The implementation was written in Python 3.10. Key software libraries and frameworks include NumPy 1.24.2, SciPy 1.10.1, scikit-learn 1.2.2, and PyTorch 2.0.1 (CPU backend). Main experiments were run locally without the use of additional distributed or cloud-based resources.

## Appendix I: Sample outputs



(a) Users unanimously preferred HCC for this input with ground truth whiptail, HCC prediction {lizard} and standard CP prediction {agama, alligator lizard, green lizard, whiptail}.



(b) Users unanimously preferred standard CP for this input with ground truth ram, HCC prediction {bovid} and standard CP prediction {ram, big horn}.



(c) Users unanimously indicated no preference for this input with ground truth tape player, HCC prediction {whole} and standard CP prediction {ashcan, ballpoint, bannister,

bookcase, carpenter's kit, carton, cash machine, cassette, cassette player, cd player, chest, chiffonier, china cabinet, combination lock, computer keyboard, crash helmet, crate, desk, desktop computer, digital clock, dishwasher, drumstick, entertainment center, envelope, file, fire screen, fountain pen, freight car, garbage truck, grille, hammer, hard disc, harmonica, home theater, hook, joystick, laptop, loudspeaker, mailbox, marimba, microwave, modem, monitor, notebook, organ, paintbrush, paper towel, pay-phone, pencil sharpener, photocopier, pickup, plate rack, polaroid camera, pool table, printer, projector, radio, recreational vehicle, refrigerator, rubber eraser, safe, scale, school bus, screwdriver, slide rule, slot, space heater, spatula, stove, tape player, television, theater curtain, toaster, tobacco shop, toilet tissue, turnstile, upright, vending machine, volleyball, wallet}.

Figure 9: Example output and user preferences for random samples from `img` with unanimous user preferences.